Available online at www.sciencedirect.com
ScienceDirect
Catalysis Today 127 (2007) 319–329
CATALYSIS TODAY
www.elsevier.com/locate/cattod

A comparative study of the water-gas shift activity of Pt catalysts supported on single (MO_x) and composite (MO_x/Al_2O_3, MO_x/TiO_2) metal oxide carriers

Paraskevi Panagiotopoulou, Dimitris I. Kondarides *

Department of Chemical Engineering, University of Patras, GR-26504 Patras, Greece

Available online 21 June 2007

Abstract

The water-gas shift (WGS) activity of platinum catalysts dispersed on a variety of single metal oxides as well as on composite MO_x/Al_2O_3 and MO_x/TiO_2 supports (M = Ti, V, Cr, Mn, Fe, Co, Ni, Cu, Y, Zr, La, Ce, Nd, Sm, Eu, Gd, Ho, Er, Tm) has been investigated in the temperature range of 150–500 °C, using a feed composition consisting of 3% CO an 10% H_2O. For Pt catalysts supported on single metal oxides, it has been found that both the apparent activation energy of the reaction and the intrinsic rate depend strongly on the nature of the support. In particular, specific activity of Pt at 250 °C is 1–2 orders of magnitude higher when supported on ''reducible'' compared to ''irreducible'' metal oxides. For composite $Pt/MO_x/Al_2O_3$ and $Pt/MO_x/TiO_2$ catalysts, it is shown that the presence of MO_x results in a shift of the CO conversion curve toward lower reaction temperatures, compared to that obtained for Pt/Al_2O_3 or Pt/TiO_2, respectively. The specific reaction rate is in most cases higher for composite catalysts and varies in a manner which depends on the nature, loading, and primary crystallite size of dispersed MO_x. Results are explained by considering that reducibility of small oxide particles increases with decreasing crystallite size, thereby resulting in enhanced WGS activity. Therefore, evidence is provided that the metal oxide support is directly involved in the WGS reaction mechanism and determines to a significant extent the catalytic performance of supported noble metal catalysts. Results of catalytic performance tests obtained under realistic feed composition, consisting of 3% CO, 10% H_2O, 20% H_2 and 6% CO_2, showed that certain composite $Pt/MO_x/Al_2O_3$ and $Pt/MO_x/TiO_2$ catalysts are promising candidates for the development of active WGS catalysts suitable for fuel cell applications.

Keywords: Water-gas shift; Platinum; Metal oxide; Composite catalysts; Reducibility

1. Introduction

The potential use of hydrogen as a future energy carrier has stimulated research for the development of fuel processors suitable for generating hydrogen for mobile and residential fuel cell applications [1–4]. Fuel processors designed for use with polymer electrolyte membrane (PEM) fuel cells should be able to convert hydrocarbon fuels into hydrogen-rich gas streams with residual carbon monoxide levels typically bellow 50 ppm. This can be accomplished by treatment of the reformate gas in a water-gas shift (WGS) unit, in order to reduce CO concentration to 0.5–1.0%, followed by a final purification step, which may involve preferential oxidation or methanation of residual CO [1–4]. The WGS reaction is moderately exothermic and equilibrium-limited and, therefore, the desired CO levels can only be achieved at low temperatures. As a result, WGS catalysts for fuel cell applications should be sufficiently active in the temperature range of 200–280 °C, thermally stable, and resistant to poisoning under the reformer's conditions. In addition, they should be characterized by high selectivity for a wide range of H_2O/CO ratios with no side reactions, particularly methanation, which would consume valuable hydrogen.

Conventional high temperature (Fe–Cr oxide) and low temperature ($Cu–Zn–Al_2O_3$) WGS catalysts, which have been practiced for several decades in large scale steady-state operations, do not meet the above criteria and, therefore, cannot be used in fuel cell applications. This has led to intensive interest in the development of novel catalyst formulations for the WGS reaction, which are based on noble metals supported on metal oxide carriers [5–18]. Among the various metal-support

* Corresponding author. Tel.: +30 2610 969527; fax: +30 2610 991527.
E-mail address: dimi@chemeng.upatras.gr (D.I. Kondarides).

0920-5861/$ – see front matter © 2007 Elsevier B.V. All rights reserved.
doi:10.1016/j.cattod.2007.05.010

combinations investigated so far, Pt/CeO_2 [12–14] and oxide-supported Au catalysts [5] have been reported to exhibit exceptionally high activity at low reaction temperatures. However, activity and stability of Au under realistic reaction conditions is questionable and depends strongly on the preparation method and pre-treatment conditions employed [5,15]. On the other hand, ceria-supported noble metal catalysts progressively deactivate under conditions typical of a reformer outlet [16]. As a result, efforts for developing novel, highly active and stable WGS catalysts at low temperatures are still in progress.

In our previous studies [17–20], we have investigated in detail the catalytic performance of oxide-supported noble metals in an attempt to identify the key physicochemical parameters, which affect WGS activity. It has been found that the specific reaction rate (TOF) does not depend on metal loading, dispersion or crystallite size [17,18], but mainly on the nature and characteristics of the support. In particular, it has been found that activity of platinum (and other noble metals) [17,18] is significantly improved when dispersed on ''reducible'' rather than on ''irreducible'' metal oxides. It was also shown that activity of Pt/TiO_2 catalysts depends strongly on the primary crystallite size of the support [17]. This behavior has been attributed to the higher reducibility of small titania crystallites, which may affect either directly (redox properties) or indirectly (population and reactivity of hydroxyl groups) the WGS activity [17,19].

Metal oxides (MO_x) with small primary particles size may be produced by dispersion of MO_x on high surface area supports, such as Al_2O_3 or SiO_2, which has been reported to result in significant enhancement of activity, selectivity and/or stability of dispersed noble metals for a number of catalytic reactions [21–32]. In the present study, the water-gas shift activity of platinum catalysts dispersed on composite MO_x/Al_2O_3 or MO_x/TiO_2 supports is investigated and results are compared to those obtained for Pt catalysts supported on the corresponding single metal oxides. The relation between WGS activity and physicochemical properties of the support is discussed.

2. Experimental

2.1. Catalyst preparation and characterization

Composite MO_x/Al_2O_3 (M = Ti, V, Cr, Mn, Fe, Co, Ni, Cu, Y, Zr, La, Ce, Nd, Sm, Eu, Gd, Ho, Er, Tm) and MO_x/TiO_2 (M = Co, Y, Ce, Nd, Gd, Ho) supports were prepared by impregnation of Al_2O_3 (Alfa Products, 90 m^2/g) or TiO_2 (Degussa P25, 50 m^2/g) powder in an aqueous solution of the corresponding metal oxide precursor salt ($Ce(NO_3)_3 \cdot 6H_2O$, $Ni(NO_3)_2 \cdot 6H_2O$, $La(NO_3)_3 \cdot 6H_2O$, $Fe(NO_3)_3 \cdot 9H_2O$,$Co(NO_3)_2 \cdot 6H_2O$, $Cr(NO_3)_3 \cdot 9H_2O$, $ZrO(NO_3)_2 \cdot 6H_2O$, $Mn(NO_3)_2 \cdot 6H_2O$, $Cu(NO_3)_2 \cdot 3H_2O$, $Tm(NO_3)_3 \cdot 5H_2O$, $Eu(NO_3)_3 \cdot 6H_2O$, $Nd(NO_3)_3 \cdot 5H_2O$, $Sm(NO_3)_3 \cdot 6H_2O$, $Ho(NO_3)_3 \cdot 5H_2O$, $Er(NO_3)_3 \cdot 5H_2O$, $Gd(NO_3)_3 \cdot 5H_2O$, $Ho(NO_3)_3 \cdot 5H_2O$, $Y(NO_3)_3 \cdot 6H_2O$ or $Ti(OC_3H_7)_4$). The resulting slurry was heated slowly at 70 °C under continuous stirring and maintained at that temperature until nearly all the water evaporated. The solid residue was dried at 110 °C for 24 h and finally calcined at 600 °C for 3 h. Unless otherwise indicated, the loading of the metal oxide (MO_x) on the Al_2O_3 or TiO_2 carrier was 10 wt.%. Selected experiments were also conducted with the use of catalysts of variable MO_x loading, in the range of 0–20 wt.%. For comparison purposes, and in order to produce materials with similar physicochemical characteristics, Al_2O_3 and TiO_2 powders were also exposed to the same preparation method (impregnation, drying and calcination at 600 °C for 3 h).

Dispersed platinum catalysts were prepared employing the wet impregnation method with the use of the above composite MO_x/Al_2O_3 and MO_x/TiO_2 carriers and $(NH_3)_2Pt(NO_2)_2$ (Alfa) as a platinum precursor salt [17]. The same method was used for the preparation of Pt catalysts supported on a variety of commercial metal oxide powders (Al_2O_3, TiO_2, CeO_2, Nd_2O_3, Y_2O_3, SiO_2, MgO, La_2O_3, Co_3O_4, Fe_2O_3, ZrO_2, Cr_2O_3, MgO). The nominal Pt loading of all catalysts thus prepared was 0.5 wt.%.

Catalysts were characterized with respect to their specific surface area, phase composition and crystallite size of the support, and exposed platinum surface area employing nitrogen physisorption at the temperature of liquid nitrogen, X-ray diffraction (XRD) and selective chemisorption of H_2 or CO, following the procedures described in detail elsewhere [17].

2.2. Catalytic performance tests and kinetic measurements

Catalytic performance tests have been carried out using an apparatus which has been described in detail elsewhere [17]. It consists of a flow measuring and control system equipped with mass-flow controllers and a syringe pump, a quartz micro reactor, and a gas chromatograph (Shimadzu) interfaced to a personal computer for on line analysis of reactants and products. The chromatograph is equipped with two packed columns (Porapak-Q, Carboxen) and two detectors (TCD, FID) and operates with He as the carrier gas. The injection of the gas mixture to the desired column is achieved by means of two six-port valves heated at 150 °C. Determination of the response factors of the detectors has been achieved with the use of gas streams of known composition (Scott specialty gas mixtures). Unless otherwise indicated, the only reaction products detected were CO_2 and H_2. Reaction gases (He, 10% CO/He, H_2, CO_2) are supplied from high-pressure gas cylinders (Messer Griesheim GMBH) and are of ultra-high purity.

Catalytic performance has been investigated in the temperature range of 100–550 °C using a feed stream consisting of 3% CO and 10% H_2O (balance He). Selected catalysts have been also tested under more realistic feed compositions consisting of 3% CO, 10% H_2O, 20% H_2 and 6% CO_2. In a typical experiment, an amount of 100 mg of fresh catalyst ($0.18 < d < 0.25$ mm) is placed in the reactor and reduced in situ at 300 °C for 1 h under a hydrogen flow of 60 cm^3/min. The catalyst is then heated at 500 °C under He flow and left at that temperature for 15 min. Finally, temperature is lowered to 450 °C and the flow is switched to the reaction mixture. The catalyst is conditioned at this

temperature for 1 h and then the concentrations of reactants and products are determined using the analysis system described above. Similar measurements are obtained following a stepwise lowering of temperature, until conversion of CO drops close to zero. All experiments were performed at near atmospheric pressure.

Measurements of intrinsic rates were obtained in separate experiments under differential reaction conditions. Results were used to determine the turnover frequencies (TOFs) of carbon monoxide, defined as the number of CO molecules converted per surface Pt metal atom per second. Details on the methods and procedures employed can be found elsewhere [17].

3. Results

3.1. Physicochemical characteristics of supported Pt catalysts

Results of catalyst characterization measurements obtained for Pt catalysts supported on commercial oxide powders are summarized in Table 1, where the specific surface area (SSA), primary crystallite size of the oxide support (d_{MO_x}), Pt dispersion and Pt mean crystallite size (d_{Pt}) are listed for the samples investigated. It is observed that SSA varies significantly from one catalyst to another, taking values between 0.4 m^2/g for Pt/MnO to 144 m^2/g for Pt/SiO_2. As a result of differences in the nature and surface area of the oxide support, Pt dispersion also varies between 6.8% and 99% (Table 1).

Physicochemical characteristics of platinum catalysts dispersed on composite MO_x/Al_2O_3 carriers are summarized in Table 2. Results of SSA measurements show that deposition of MO_x results in catalysts with decreased surface areas, compared to that of Pt/Al_2O_3. This is most probably caused by blocking of the pores of the Al_2O_3 support by the crystallites of dispersed metal oxides. It should be noted, however, that the specific surface area of $Pt/MO_x/Al_2O_3$ catalysts is generally much higher, compared to that of Pt supported on commercial metal oxides. Dispersion of Pt over this set of catalysts takes values typically higher than 20% (Table 2). Similar results obtained for $Pt/MO_x/TiO_2$ catalysts are listed in Table 3.

X-ray diffraction spectra were obtained for all freshly prepared (H_2-reduced) catalysts investigated. It has been found that, in most cases, diffractograms obtained for $Pt/MO_x/Al_2O_3$ and $Pt/MO_x/TiO_2$ samples contain only peaks attributable to Al_2O_3 or TiO_2, respectively. This indicates that MO_x species are characterized by low crystallinity and/or high dispersion (small crystallite size). However, for certain $Pt/MO_x/Al_2O_3$ catalysts shown in Fig. 1 (M = Ce, Ti, La, Ni, Fe, Mn, Cu), additional XRD peaks appear in the diffractograms due to the presence of the corresponding MO_x crystallites. For these samples, the primary crystallite size of MO_x was estimated from X-ray line broadening with the use of the Sheerrer equation [17] and results are shown in Table 2. Estimation of d_{MO_x} was not possible for the rest of the H_2-reduced composite catalysts investigated. It should be noted that for spectra shown in Fig. 1, diffraction peaks assigned to MO_x correspond to oxide phases. An exception is observed for $Pt/CuO_x/Al_2O_3$ catalyst, for which XRD peaks obtained for the freshly prepared (H_2-reduced) sample correspond to metallic Cu. However, the XRD spectrum obtained from the preoxidized sample (not shown for brevity) exhibited lines assigned to CuO. Regarding the Co-containing samples, although XRD patterns of the freshly prepared catalysts did not contain peaks attributable to CoO_x, the spectra obtained from the pre-oxidized samples contained peaks assigned to Co_3O_4. Values of $d_{Co_3O_4}$ determined from the latter experiments are shown in Table 2.

3.2. Catalytic performance of platinum supported on single metal oxides

Results of catalytic performance tests obtained over Pt catalysts supported on commercial metal oxide powders are

Table 1
Results of catalyst characterization and kinetic measurements obtained for Pt (0.5 wt.%) catalysts supported on commercial metal oxides

Oxide support	SSA[a] (m^2/g)	d (MO_x)[b] (nm)	Pt dispersion (%)	d (Pt)[c] (nm)	Rate at 250 °C		E_a[d] (kcal/mol)
					μmol s^{-1} g^{-1}	TOF (s^{-1})	
Al_2O_3	83	6	84	1.2	0.49	0.02	19.2
TiO_2	41	23	87	1.2	10.3	0.46	15.7
CeO_2	3.3	30	49	2.1	4.9	0.40	21.4
Nd_2O_3	12	16	36	2.9	2.0	0.22	22.9
Y_2O_3	5.6	–	40	2.5	0.67	0.07	23.2
SiO_2	144	–	99	1.0	0.14	0.005	13.9
MnO	0.4	25	18	5.7	0.05	0.009	27.4
La_2O_3	7.0	–	23	4.4	1.15	0.20	24.6
Co_3O_4	1.3	17	6.8	15.1	0.46	0.26	34.1
Fe_2O_3	7.3	17	56	1.8	0.03	0.002	24.6
ZrO_2	4.0	–	18	5.6	1.31	0.28	19.6
Cr_2O_3	5.7	–	15	6.8	0.40	0.10	14.8
MgO	22	17	54	1.9	0.15	0.01	17.2

[a] Specific surface area, estimated with the BET method.
[b] Primary crystallite size of MO_x, estimated from XRD line broadening.
[c] Mean crystallite size of platinum, estimated from selective chemisorption measurements.
[d] Apparent activation energy.

Table 2
Results of catalyst characterization and kinetic measurements obtained for the investigated 0.5% $Pt/MO_x/Al_2O_3$ catalysts

MO_x		SSA[a] (m^2/g)	d (MO_x)[b] (nm)	Pt dispersion (%)	d (Pt)[c] (nm)	Rate at 250 °C		E_a[d] (kcal/mol)
M	Loading (wt.%)					μmol s^{-1} g^{-1}	TOF (s^{-1})	
None (Al_2O_3)	–	88	–	84	1.2	0.49	0.02	19.2
Ti	10	86	7	100	1.0	3.16	0.12	15.4
V	10	97	n.d.[e]	24	4.3	0.99	0.17	18.3
Cr	10	71	n.d.	65	1.6	0.58	0.04	19.8
Mn	10	71	17	81	1.3	0.55	0.03	17.8
Fe	10	72	10	32	3.2	0.61	0.07	21.9
Co	5	75	15[f]	77	1.3	1.72	0.09	22.1
	10	64	10[f]	91	1.1	3.66	0.14	24.2
	20	56	15[f]	100	1.0	3.23	0.13	24.6
Ni	10	65	8	100	1.0	1.50	0.06	21.7
Cu	10	66	20	100	1.0	2.22	0.09	12.2
Y	10	52	n.d.	17	6.0	1.83	0.41	20.0
Zr	10	73	n.d.	54	1.9	1.87	0.12	17.5
La	10	55	7	54	1.9	1.76	0.15	21.0
Ce	10	68	8	71	1.4	4.84	0.28	21.8
Nd	10	57	n.d.	12	8.5	2.23	0.73	19.2
Sm	10	60	n.d.	26	3.9	1.31	0.20	16.9
Eu	10	61	n.d.	17	6.0	1.85	0.43	19.7
Gd	10	56	n.d.	21	4.8	1.88	0.34	22.5
Ho	10	58	n.d.	21	4.8	2.57	0.48	20.8
Er	10	60	n.d.	24	4.2	0.83	0.13	20.2
Tm	10	60	n.d.	19	5.5	1.19	0.25	19.9

[a] Specific surface area, estimated with the BET method.
[b] Primary crystallite size of MO_x, estimated from XRD line broadening.
[c] Mean crystallite size of platinum, estimated from selective chemisorption measurements.
[d] Apparent activation energy.
[e] n.d.: MO_x not detected by XRD.
[f] Results obtained over pre-oxidized catalysts (see text).

shown in Fig. 2, where conversion of CO (X_{CO}) is plotted as a function of reaction temperature, for each sample investigated. The equilibrium conversion predicted by thermodynamics is also shown, for comparison. It is observed that, under the present experimental conditions, Pt/TiO_2 is the most active catalyst at low temperatures, exhibiting measurable CO conversion at temperatures as low as 150 °C. Conversion of CO increases with increasing temperature and reaches equilibrium at ca. 380 °C. Platinum catalysts supported on Nd_2O_3, La_2O_3 or CeO_2 become active at temperatures higher

Table 3
Results of catalyst characterization and kinetic measurements obtained for the investigated 0.5% $Pt/MO_x/TiO_2$ catalysts

MO_x		SSA[a] (m^2/g)	d (MO_x)[b] (nm)	Pt dispersion (%)	d (Pt)[c] (nm)	Rate at 250 °C		E_a[d] (kcal/mol)
M	Loading (wt.%)					μmol s^{-1} g^{-1}	TOF (s^{-1})	
None (TiO_2)	–	41	23	87	1.2	10.3	0.46	15.7
Co	10	29	n.d.[e]	97	1.0	8.3	0.33	15.8
Y	10	37	n.d.	67	1.5	4.8	0.28	15.6
Ce	2	–	–	100	1.0	18.2	0.70	15.4
	5	36	–	63	1.6	19.4	1.19	17.9
	10	37	6.8	100	1.0	21.1	0.83	19.4
	20	–	–	100	1.0	19.6	0.77	20.8
Nd	5	37	–	83	1.2	15.6	0.73	15.6
	10	35	n.d.	64	1.6	14.7	0.88	15.6
Gd	10	38	n.d.	100	0.9	11.4	0.45	17.3
Ho	10	36	n.d.	59	1.7	8.9	0.59	17.2

[a] Specific surface area, estimated with the BET method.
[b] Primary crystallite size of MO_x, estimated from XRD line broadening.
[c] Mean crystallite size of platinum, estimated from selective chemisorption measurements.
[d] Apparent activation energy.
[e] n.d.: MO_x not detected by XRD.

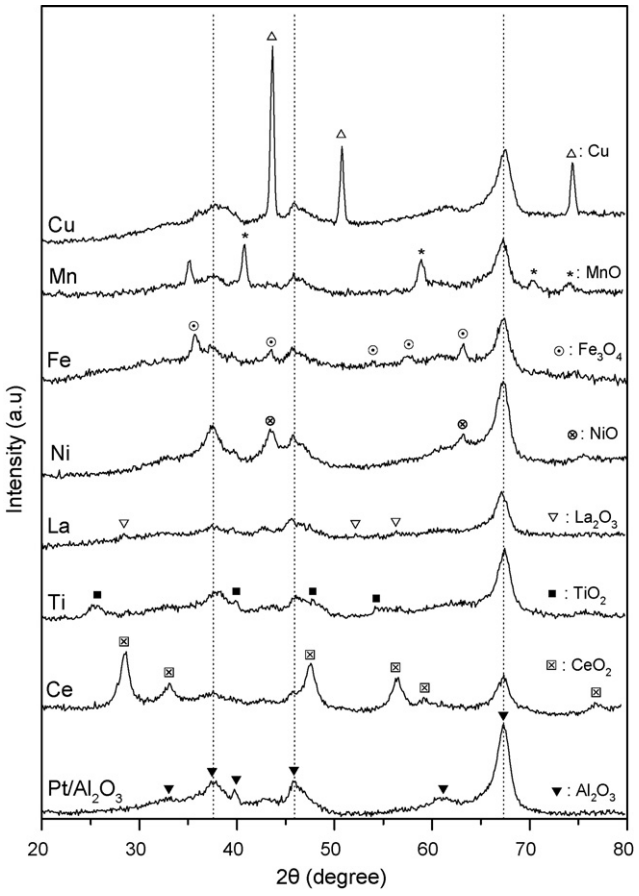

Fig. 1. XRD patterns obtained from reduced 0.5% Pt/Al_2O_3 and 0.5% Pt/10% MO_x/Al_2O_3 catalysts (M = Ce, Ti, La, Ni, Fe, Mn, Cu).

than 200 °C and reach equilibrium above 400 °C, while Y_2O_3- and Al_2O_3-supported catalysts become active at sufficiently higher temperatures. MgO- and SiO_2-supported platinum catalysts are practically inactive in the temperature range of interest, since temperatures higher than 450 °C are required in order to achieve conversions above 20%. The Pt/Co_3O_4 catalyst, although not very active at temperatures below 250 °C, is able to reach equilibrium CO conversion at 350 °C, i.e., at the lowest temperature among this set of catalysts (Fig. 2).

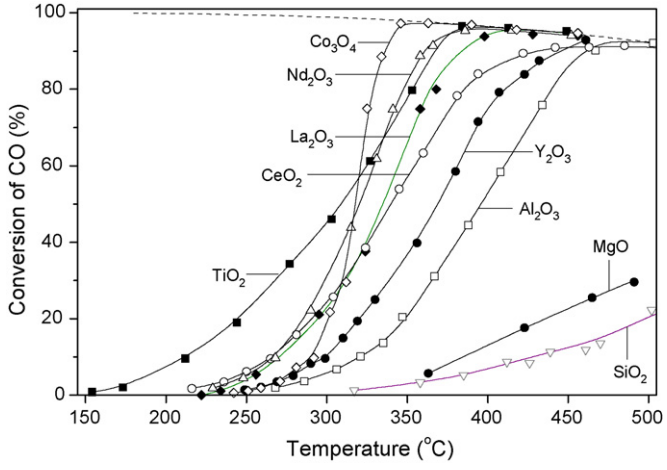

Fig. 2. Conversion of CO as a function of reaction temperature obtained over Pt (0.5 wt.%) catalysts dispersed on the indicated metal oxides. Equilibrium conversion is shown with dashed line. *Experimental conditions*: mass of catalyst: 100 mg; particle diameter: $0.18 < d_p < 0.25$ mm; feed composition: 3% CO + 10% H_2O (balance: He); total flow rate: 200 cm^3/min.

The intrinsic activity of the above Pt/metal oxide catalysts has been measured under differential reaction conditions in the temperature range of 200–350 °C. Representative results are summarized in Table 1, where the specific reaction rate at 250 °C (expressed both per gram of catalyst and per exposed Pt atom) as well as the apparent activation energy (E_a) of the reaction, estimated from the corresponding Arrhenius plots (e.g., Figs. 4 and 6, vide infra), are listed for all samples investigated. It is observed that the reaction rate depends strongly on the nature of the oxide support, with Pt being ca. two orders of magnitude more active when supported on TiO_2 (0.46 s^{-1}) than on SiO_2 (0.005 s^{-1}). The nature of the support also affects significantly the activation energy of the reaction, which varies between 13.9 kcal/mol for Pt/SiO_2 and 34.1 kcal/mol for Pt/Co_3O_4 catalysts (Table 1).

3.3. WGS activity of $Pt/MO_x/Al_2O_3$ catalysts

The effect of deposition of metal oxides on the Al_2O_3 support on the catalytic activity of dispersed Pt has been investigated with the use of catalysts with the same MO_x loading (10 wt.%). Results of catalytic performance tests obtained with the use of oxides of the 3d transition metal elements are presented in Fig. 3A. The catalytic performance of Pt/Al_2O_3 is also shown, for comparison. It is observed that, with the exception of the Mn-containing sample, addition of MO_x results in a shift of the CO conversion curve toward lower reaction temperatures, compared to that obtained for Pt/Al_2O_3. This shift is more pronounced for Ni-, Ti- and, especially, Co-containing samples and less important for Fe- or Cr-containing catalysts. Best results are obtained over the $Pt/CoO_x/Al_2O_3$ catalyst, which is able to reach equilibrium CO conversion at about 330 °C, i.e., at a temperature which is lower by ca. 20 or 150 °C, compared to that obtained over the corresponding single component Pt/Co_3O_4 or Pt/Al_2O_3 catalysts, respectively (compare with the corresponding curves in Fig. 2). The $Pt/TiO_x/Al_2O_3$ catalyst exhibits high CO conversions at temperatures below 300 °C but reaches equilibrium above 440 °C (Fig. 3A). In general, the catalytic performance of the latter sample is inferior, compared to that obtained for the single component Pt/TiO_2 catalyst (Fig. 2). The $Pt/CuO_x/Al_2O_3$ catalyst is comparably active at low temperatures, but X_{CO} increases slowly with temperature, making this sample the least active one at high temperatures, compared to other $Pt/MO_x/Al_2O_3$ catalysts investigated (Fig. 3A). Qualitatively similar is the performance of the V-containing catalyst (not shown for clarity), which becomes active at ca. 250 °C and does not reach equilibrium conversion at temperatures up to 500 °C.

Deposition of oxides of the 4d transition metal elements (Y, Zr) on Al_2O_3 also resuls in $Pt/MO_x/Al_2O_3$ catalysts with superior WGS performance, compared to that of Pt/Al_2O_3. The corresponding CO conversion curves (not shown for brevity) lie

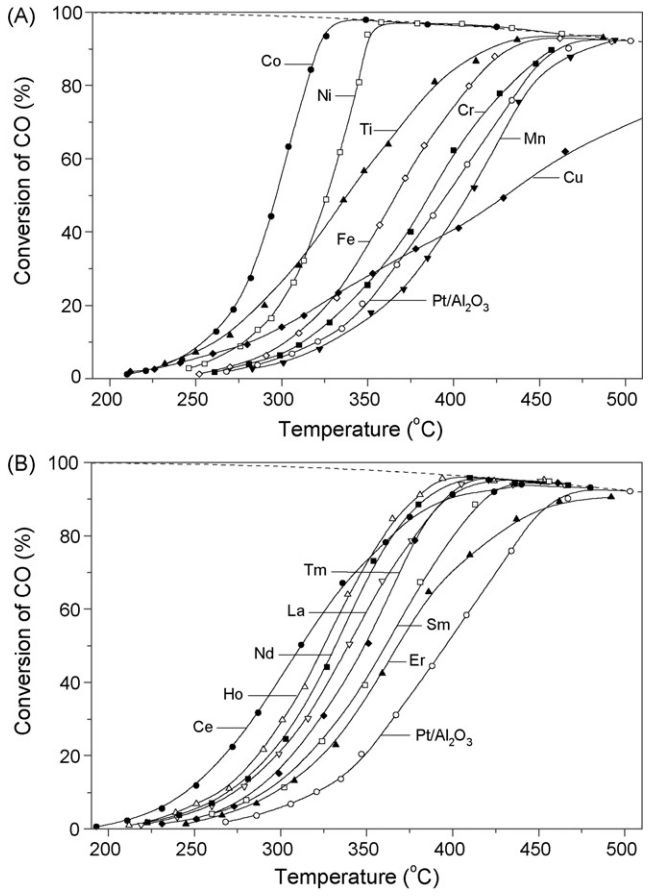

Fig. 3. Conversion of CO as a function of reaction temperature obtained over 0.5% $Pt/MO_x/Al_2O_3$ catalysts, for M belonging to (A) 3d transition metal elements and (B) rare earth metals. The conversion curve obtained for 0.5% Pt/Al_2O_3 is also shown, for comparison. MO_x loading: 10 wt.%. *Experimental conditions*: same as in Fig. 2.

between those obtained for the Ti- and Fe-containing samples (Fig. 3A).

Results of catalytic performance tests obtained following addition of rare earth metal oxides (M = La, Ce, Nd, Sm, Eu, Gd, Ho, Er, Tm) on the alumina carrier are shown in Fig. 3B. It is observed that, in all cases, the CO conversion curve shifts toward lower temperatures in the presence of MO_x, compared to that obtained for Pt/Al_2O_3. Under the present experimental conditions, the Ce-containing sample is the most active one at temperatures lower than ca. 350 °C, whereas the Ho-containing catalyst reaches equilibrium conversion at ca. 400 °C, i.e., at the lowest temperature among catalyst samples of this series. The CO conversion curves of Eu- and Gd-containing catalysts (not shown for clarity) fall between those obtained for the Nd- and La-containing samples (Fig. 3B).

The intrinsic reaction rate has been measured under differential reaction conditions for all $Pt/MeO_x/Al_2O_3$ catalysts investigated and representative results obtained for Co-, Nd- and Ti-containing samples are shown in the Arrhenius plots of Fig. 4. The reaction rates at 250 °C as well as values of the apparent activation energy (E_a) of the reaction for all samples investigated are summarized in Table 2. It is observed that the specific rate (per gram of catalyst) at 250 °C depends

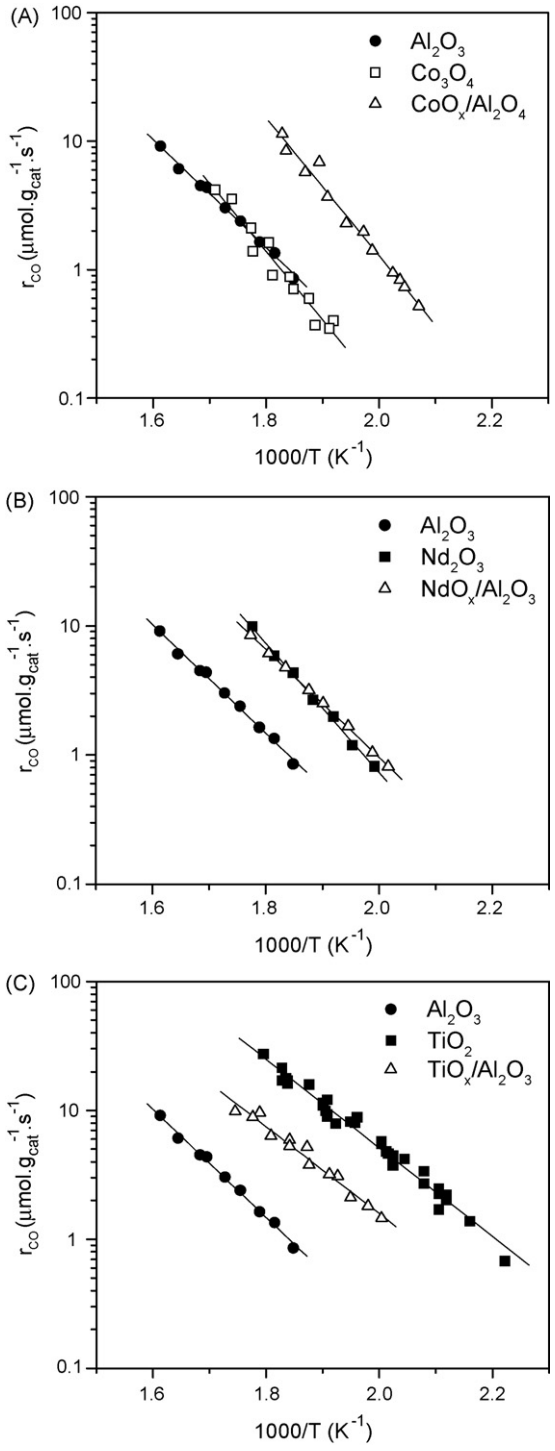

Fig. 4. Arrhenius plots of rates of CO conversion obtained over Pt (0.5 wt.%) catalysts supported on (A) CoO_x/Al_2O_3, (B) NdO_x/Al_2O_3 and (C) TiO_x/Al_2O_3. Rates of Pt supported on the corresponding single oxides are also shown, for comparison.

strongly on the nature of MO_x and is in all cases higher than that obtained for Pt/Al_2O_3. In particular, activity at 250 °C varies, depending on the nature of M in MO_x, in the order of Ce > Co > Ti > Ho > Nd ≈ Cu > Gd ≈ La ≈ Eu ≈ Y ≈ Zr > Ni > Sm > Tm > V > Er > Fe > Cr ≈ Mn > Al_2O_3, with the rate for $Pt/CeO_x/Al_2O_3$ catalyst being about one order of magnitude higher than that of Pt/Al_2O_3, at 250 °C. At higher

temperatures the above order of activity is somewhat different due to variations in E_a, which ranges between 12.2 kcal/mol for $Pt/CuO_x/Al_2O_3$ and 24.5 kcal/mol for $Pt/CoO_x/Al_2O_3$ (Table 2).

It is of interest to note that for most of the $Pt/MO_x/Al_2O_3$ catalysts investigated, the reaction rate per gram of catalyst is not only higher compared to that obtained for Pt/Al_2O_3 but also compared to that obtained for the corresponding Pt/MO_x catalyst. This is, for example, the case for M = Co (Fig. 4A), La, Fe, Zr, Cr and Y. In other cases, e.g., for M = Nd (Fig. 4B), Ce and Mn, the rate is practically the same for $Pt/MO_x/Al_2O_3$ and Pt/MO_x catalysts. Finally, the activity of $Pt/TiO_x/Al_2O_3$ catalyst is significantly lower, compared to that of Pt/TiO_2 (Fig. 4C). Since all $Pt/MO_x/Al_2O_3$ catalysts investigated have comparable specific surface areas (Table 2), the observed differences in WGS activity should not be attributed to the possible effect SSA on catalytic performance but on the presence of dispersed MO_x species.

If specific reaction rates are expressed per exposed Pt atom (TOF), the $Pt/MO_x/Al_2O_3$ catalysts containing rare-earth metal oxides are generally much more active, compared to those containing oxides of the 3d transition metal elements (Table 2). For example, TOFs over catalysts containing Nd (0.73 s^{-1}), Ho (0.48 s^{-1}) or Eu (0.43 s^{-1}) are about one order of magnitude higher, compared to those obtained for samples containing Ti (0.12 s^{-1}), Fe (0.07 s^{-1}), Cr (0.04 s^{-1}) or Mn (0.03 s^{-1}) (Table 2). It should be noted, however, that the exposed surface area of Pt, determined by selective chemisorption of hydrogen (or CO) at 25 °C, may have been overestimated for the latter set of catalysts due to spillover and/or adsorption of the probe molecule on the MO_x-containing support.

3.4. WGS activity of $Pt/MO_x/TiO_2$ catalysts

Results of our present (Fig. 2) and previous [17–19] studies clearly show that platinum catalysts exhibit exceptionally high activity at temperatures lower than 300 °C when supported on TiO_2, compared to other metal oxides. In order to investigate if the performance of TiO_2-based catalysts can be further improved, oxides of selected metals (M = Ce, Nd, Co, Ho, Y, Gd) were also deposited on TiO_2 (Degussa P25) and tested for their WGS activity. Results of catalytic performance tests are shown in Fig. 5, where X_{CO} is plotted as a function of reaction temperature for all $Pt/MO_x/TiO_2$ samples studied. It is observed that addition of Ho, Gd and, especially Ce or Nd on TiO_2 results in a shift of the conversion curves toward lower reaction temperatures, compared to that obtained for Pt/TiO_2. The same is true for $Pt/CoO_x/TiO_2$ catalyst, the conversion curve of which (not shown for clarity) lies between those obtained for Gd- and Ho-containing samples. In contrast, deposition of YO_x did not result in an improvement of catalytic performance (Fig. 5). Comparison of CO conversion curves presented in Figs. 3 and 5 shows that, in general, $Pt/MO_x/TiO_2$ catalysts exhibit higher CO conversions at a given temperature, compared to those of $Pt/MO_x/Al_2O_3$ samples of the same MO_x nature and loading.

The intrinsic reaction rate has been measured under differential reaction conditions for all $Pt/MO_x/TiO_2$ samples investigated. Representative results obtained for catalysts with

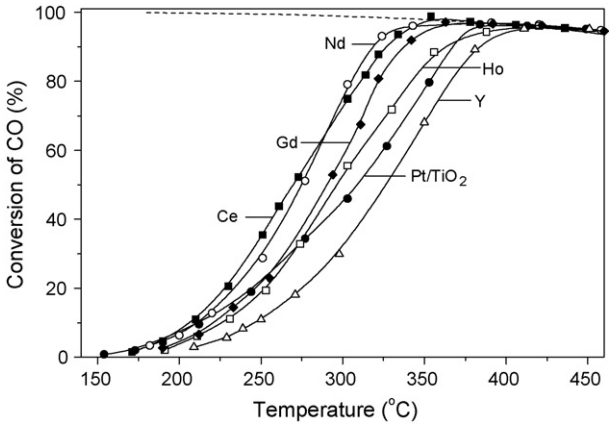

Fig. 5. Conversion of CO as a function of reaction temperature obtained over 0.5% $Pt/MO_x/TiO_2$ catalysts, for M = Ce, Gd, Nd, Ho and Y. The conversion curve obtained for 0.5% Pt/TiO_2 is also shown, for comparison. MO_x loading: 10 wt.%. *Experimental conditions*: same as in Fig. 2.

M = Co, Nd or Ce are shown in the Arrhenius plots of Fig. 6, while apparent activation energies and reaction rates obtained at 250 °C are summarized in Table 3, for all catalyst samples of this series. It is observed that specific activity increases for Nd- and Ce-containing samples (Fig. 6B and C), it is not significantly affected for the Co-(Fig. 6A), Ho- and Gd-loaded catalysts and is lower for $Pt/YO_x/TiO_2$, compared to Pt/TiO_2 (Table 3). The apparent activation energy (E_a) of the reaction does not vary significantly, taking values between 15.6 and 19.4 kcal mol^{-1} for the samples containing 10% MO_x (Table 3).

3.5. Effect of MO_x loading on WGS activity

The effect of MO_x loading on the catalytic performance has been investigated over Pt catalysts supported on selected MO_x/Al_2O_3 (M = Co, Ce) and MO_x/TiO_2 (M = Ce, Nd) carriers and typical results obtained are shown in Fig. 7. It is observed that in the case of $Pt/CoO_x/Al_2O_3$ catalysts (Fig. 7A) increasing CoO_x content from 5% to 20% results in a shift of the CO conversion curve toward progressively lower temperatures. It is of interest to note that, in all cases, the $Pt/CoO_x/Al_2O_3$ catalysts exhibit a significantly improved WGS performance, compared to that obtained for single component Pt/Co_3O_4 or Pt/Al_2O_3 catalysts. A similar behavior has been observed for $Pt/CeO_x/Al_2O_3$ catalysts (not shown for brevity), where optimal results were obtained for the sample containing 10% CeO_x.

Qualitatively similar results were obtained for $Pt/CeO_x/TiO_2$ and $Pt/NdO_x/TiO_2$ catalysts of variable MO_x content. As observed in Fig. 7B, the CO conversion curve of $Pt/CeO_x/TiO_2$ samples progressively shifts toward lower temperatures with increasing CeO_x loading from 0% to 5% but catalytic performance is not improved upon further increasing CeO_x content up to 20%.

3.6. Catalytic performance under realistic reaction conditions

Results presented in Figs. 2–7 were obtained using a feed composition consisting of 3% CO and 10% H_2O in He. Since

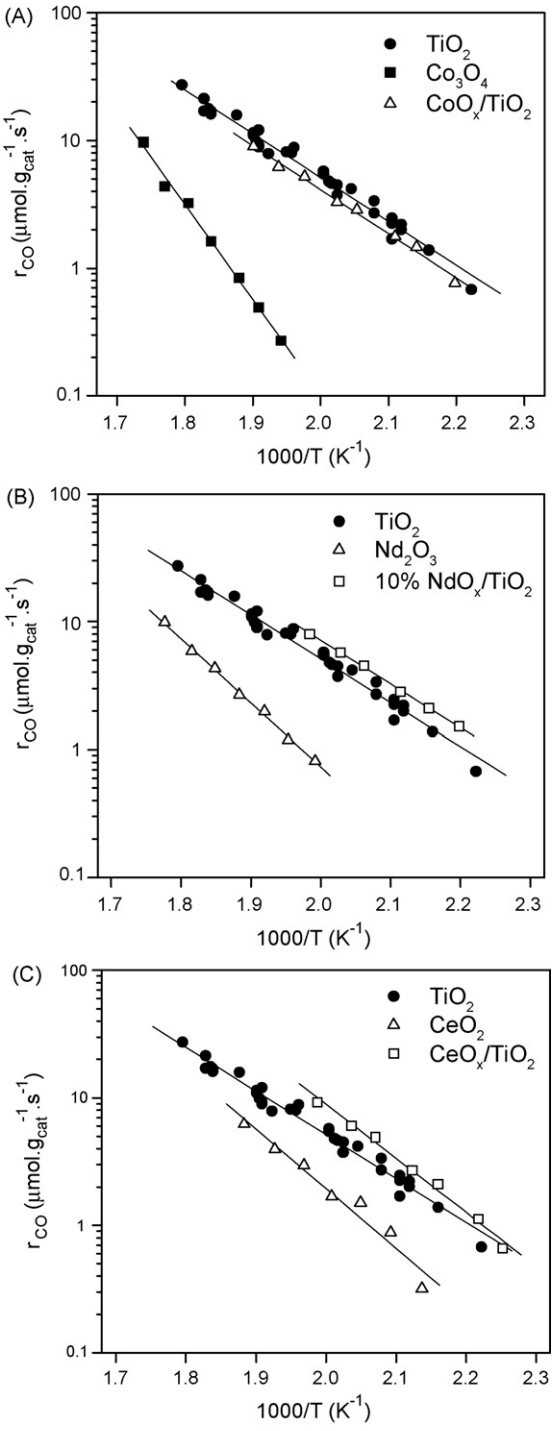

Fig. 6. Arrhenius plots of rates of CO conversion obtained over Pt (0.5 wt.%) catalysts supported on (A) CoO_x/TiO_2, (B) NdO_x/TiO_2 and (C) CeO_x/TiO_2. Rates of Pt supported on the corresponding single oxides are also shown, for comparison.

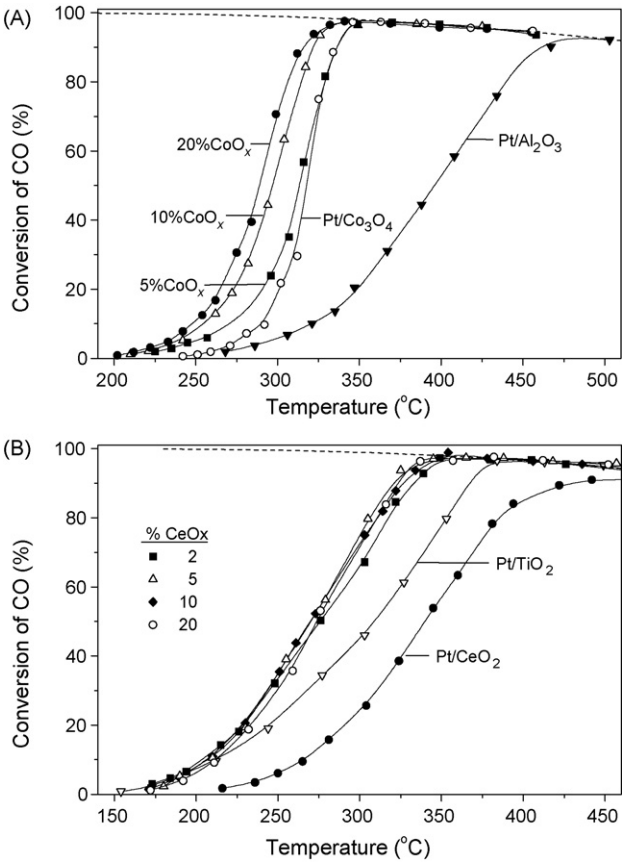

Fig. 7. Effect of MO_x loading on the catalytic performance of (A) 0.5% Pt/CoO_x/Al_2O_3 and (B) 0.5% Pt/CeO_x/TiO_2 catalysts. Conversion curves obtained for Pt supported on the corresponding single oxides are also shown, for comparison. *Experimental conditions*: same as in Fig. 2.

the effluent of fuel processors contains significant amounts of hydrogen and carbon dioxide, the catalytic performance of the prepared catalysts was also investigated under more realistic feed compositions, i.e., in the presence of 20% H_2 and 6% CO_2. Typical results of catalytic performance tests obtained for Pt catalysts supported on Al_2O_3, CeO_x/Al_2O_3, TiO_2, NdO_x/TiO_2 and CeO_x/TiO_2 are shown in Fig. 8A. Results of kinetic measurements obtained for the same catalysts are shown in the Arrhenius plots of Fig. 8B. It is observed that addition of CeO_x on the Al_2O_3-based catalyst results in a significant enhancement of X_{CO} and in a shift of the CO conversion curve toward lower temperatures (Fig. 8A). The beneficial effect of CeO_x on catalytic activity is clearly evidenced by the increase of the reaction rate by about one order of magnitude, compared to Pt/Al_2O_3 (Fig. 8B).

Under the present experimental conditions, best results were obtained for Pt/NdO_x/TiO_2 and Pt/CeO_x/TiO_2 catalysts (Fig. 8A), the activity of which is about four times higher, compared to that of Pt/TiO_2, at 300 °C (Fig. 8B). It should be noted that CoO_x- and NiO_x-containing catalysts, which were amongst the most active samples in the absence of CO_2 and H_2 in the feed (e.g., Fig. 3A), were found to promote methanation reactions in the presence of H_2 and therefore are not suitable WGS catalysts for practical applications.

Comparison of results obtained in the absence (Figs. 2–7; Tables 1–3) and in the presence of H_2 and CO_2 in the feed (Fig. 8) leads to the following two observations: first, the WGS activity of all samples is significantly suppressed in the presence of reactants in the feed. In particular, the conversion curves of CO shift to substantially higher temperatures, while the specific reaction rate decreases by about one order of magnitude in the presence of hydrogen in the feed (separate

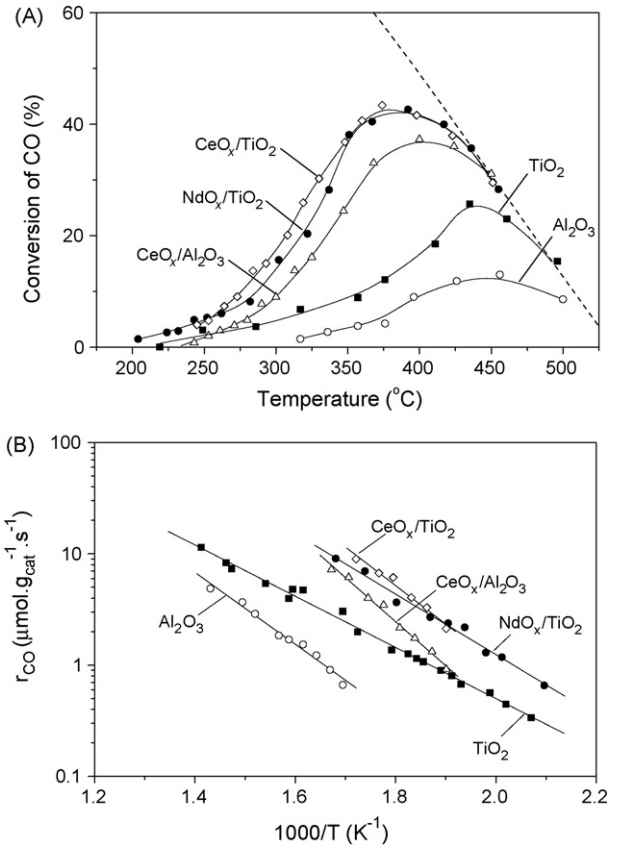

Fig. 8. (A) Conversion of CO as a function of reaction temperature and (B) Arrhenius plot of reaction rates, obtained for Pt (0.5 wt.%) catalysts supported on Al_2O_3, CeO_x/Al_2O_3, TiO_2, NdO_x/TiO_2 and CeO_x/TiO_2. *Experimental conditions*: Feed composition: 3% CO, 10% H_2O, 6CO_2, 20% H_2 (balance: He), other same as in Fig. 2.

experiments showed that the presence of CO_2 does not practically affect reaction rate). Second, the beneficial effect of addition of MO_x is more pronounced under realistic feed compositions. For example, differences in reaction rates observed for Pt/TiO_2 and $Pt/NdO_x/TiO_2$ or $Pt/CeO_x/TiO_2$ catalysts are more striking in the presence than in the absence of H_2 and CO_2 in the feed (compare Figs. 6B and 8B).

4. Discussion

Results of catalytic performance tests (Fig. 2) and kinetic measurements (Table 1) obtained over Pt catalysts dispersed on commercial metal oxide powders show that both the WGS activity and the apparent activation energy of the reaction depend strongly on the nature of the support. Moreover, it is observed that activity is generally improved when Pt is dispersed on ''reducible'' (e.g., TiO_2, CeO_2, Co_3O_4, Nd_2O_3), compared to ''irreducible'' (e.g., Al_2O_3, MgO, SiO_2) metal oxides, in agreement with the findings of our previous study [18]. The reason for this behavior may be understood by considering the potential role of the oxide support on the WGS reaction mechanism. It is generally accepted that the reaction over supported noble catalysts occurs in a bifunctional manner, with the participation of both the dispersed metallic phase, which is mainly responsible for adsorption/activation of CO, and of the metal oxide support, which is mainly responsible for adsorption/activation of H_2O. In particular, the oxide support is believed to participate in the WGS reaction either directly, via a regenerative (redox) mechanism [12,33,34], or indirectly, via an associative (formate) mechanism [35,36]. In this respect, results obtained over the investigated $Pt/MO_x/Al_2O_3$ and $Pt/MO_x/TiO_2$ catalysts will be discussed with respect to the possible effects of the presence and nature of MO_x on their redox and chemisorptive properties.

A distinction should be first made between $Pt/MO_x/Al_2O_3$ and $Pt/MO_x/TiO_2$ catalysts, based on the fact that activity of platinum is significantly lower when dispersed on bare alumina, compared to bare titania, especially at low temperatures (Fig. 2). Therefore, the effect of MO_x on catalytic activity is more pronounced for the former set of catalysts, where a relatively ''inert'' carrier is employed. It should be also noted that, although platinum dispersion (or Pt crystallite size) varies to some extent from one catalyst to another for both $Pt/MO_x/Al_2O_3$ (Table 2) and $Pt/MO_x/TiO_2$ (Table 3) catalysts, the observed differences in activity should not be attributed to effects of this parameter. This is because in our previous studies it was clearly shown that the specific reaction rate (TOF) does not practically depend on the characteristics of the dispersed metallic phase such as metal loading, dispersion or crystallite size, for a number of metal-support combinations investigated, including Pt/TiO_2, Ru/TiO_2, Pt/CeO_2 and Pt/Al_2O_3 [17,18]. Therefore, the observed differences in catalytic performance of the present $Pt/MO_x/Al_2O_3$ and $Pt/MO_x/TiO_2$ catalysts should be mainly attributed to the presence of MO_x.

For $Pt/MO_x/Al_2O_3$ catalysts, results presented in Figs. 3 and 4 and Table 2 show that addition of MO_x results in all cases in enhanced WGS activities, compared to that obtained for Pt/Al_2O_3. Similar effects have been frequently observed for a number of catalytic reactions [21–32] including oxidation of CO or CH_4 [21,22], reduction of NO by propene [23], reduction of N_2O by hydrogen or CO [24] and CO_2 reforming of CH_4 [25]. The improved catalytic performance induced by the presence of MO_x has been attributed to several factors, including increased reducibility of the support [25,27,28], stabilization of noble metal crystallites against sintering [21,24] and/or creation of new active sites at the metal-support interface [21,25,26,29,37]. For example, Mergler et al. [27] demonstrated that partially reduced metal oxides (CoO_x, MnO_x, CeO_x) are necessary to increase the activity of Pt/SiO_2 and Pt/Al_2O_3 catalysts in the CO/O_2 reaction. Similarly, the beneficial effect of addition of CoO_x on the three-way catalytic activity of Pd/Al_2O_3 has been attributed to the presence of oxidizable/reducible cobalt sites which are predominantly active for oxidation of CO and C_3H_6, hence promoting the reduction of NO [28].

The enhancement of the WGS activity of Pt/Al_2O_3 catalysts upon addition of MO_x crystallites may be explained based on the clear relation between support reducibility and WGS activity discussed above. When platinum is dispersed on composite MO_x/Al_2O_3 carriers, a fraction of Pt crystallites is expected to be in direct contact with reducible MO_x species. It

may then be suggested that this fraction should be responsible for the higher activity of $Pt/MO_x/Al_2O_3$ catalysts at low temperatures, compared to Pt/Al_2O_3 (Figs. 3 and 4; Table 2). The improvement of catalytic performance observed with increasing MO_x loading (Fig. 4A) may then be explained, since increasing MO_x content should result in an increased fraction of Pt crystallites, which are in direct contact with MO_x. However, this model can not explain the observation that, in several cases (e.g., for M = Nd, Co, Fe), the specific activity of $Pt/MO_x/Al_2O_3$ catalysts is not only higher compared to that of Pt/Al_2O_3, but also compared to that of the corresponding Pt/MO_x catalysts (Fig. 4A; Tables 1 and 2). This finding can be understood by considering the possible effects of the mean crystallite size of MO_x on WGS activity, as discussed below.

Results of XRD experiments show that for all $Pt/MO_x/Al_2O_3$ and $Pt/MO_x/TiO_2$ catalysts investigated, MO_x species are very well dispersed on Al_2O_3 or TiO_2, respectively. This is evidenced by the fact that diffraction peaks attributable to MO_x could not be detected for most samples (Tables 2 and 3). This implies that the primary crystallite size of MO_x is generally much smaller when dispersed on Al_2O_3 or TiO_2, compared to that of the corresponding single metal oxides. Calculations of Cordatos et al. [38] have shown that the reducibility of small oxide clusters depends on its size [38], as has been found, for example, in the cases of ceria [33,38] and lanthana [39]. In our previous study [17], it was clearly shown that for Pt/TiO_2 catalysts, the primary crystallite size of the support affects significantly the WGS activity, with TOF increasing by about two orders of magnitude with decreasing the primary crystallite of the support from 35 to 16 nm. This has been related to the higher reducibility of small TiO_2 crystallites [17,19], which may affect either directly (redox properties) or indirectly (population and reactivity of hydroxyl groups) the WGS activity. Based on the above, it is argued that the higher activity of $Pt/MO_x/Al_2O_3$ catalysts, compared to that of the corresponding Pt/MO_x samples (e.g., for M = Nd, Co, etc.) originates from the lower particle size of MO_x in the former set of catalysts. This argument may also explain the observation that activity reaches a plateau with increasing MO_x loading above a certain value, e.g., 10% CoO_x for $Pt/CoO_x/Al_2O_3$ catalysts (Fig. 7A; Table 2). It is reasonable to suggest that at this loading, the beneficial effect of increasing the fraction of Pt crystallites in contact with MO_x is compensated by the counteracting effect of increasing MO_x crystallite size.

The same reasoning may be used to explain results obtained for $Pt/MO_x/TiO_2$ catalysts. However, in this case addition of MO_x does not induce a pronounced effect on WGS activity, because bare TiO_2 itself is an active support. Even so, activity of Pt/TiO_2 is improved in the presence of small NdO_x (Fig. 6B), CeO_x (Fig. 6C) of GdO_x (Table 3) crystallites. For $Pt/CeO_x/TiO_2$ catalysts, the rate increases with increasing CeO_x and reaches a plateau for 10% CeO_x (Table 3). It is of interest to note that for the latter set of catalysts the apparent activation energy increases from 15.4 to 20.8 kcal/mol with increasing CeO_x loading from 2 to 20 wt.% (Table 3). Comparison with values of E_a measured for Pt supported on the corresponding single oxides (Table 1) shows that activation energy progressively shifts from that corresponding to Pt/TiO_2 (15.7 kcal/mol) to that corresponding to Pt/CeO_2 (21 kcal/mol, Table 2), with increasing CeO_x content. This finding supports the argument made above that increasing MO_x loading results in an increase of the fraction of Pt crystallites, which are in contact with MO_x.

As mentioned above, it is possible that addition of MO_x may also affect the chemisorptive properties of the supported noble metal by altering the chemisorption strength and/or by creating new active sites. For example, Noronha et al. [29] found that MO_x addition on Pd/Al_2O_3 catalysts affected the adsorptive properties of Pd toward H_2 and CO. In particular, addition of MO_x resulted in suppression of hydrogen chemisorption capacity and CO stoichiometry (bridged versus linear CO), especially for MoO_x- and NbO_x-containing catalysts [29]. Serre et al. [37] attributed the much higher activity of $Pt/CeO_2/Al_2O_3$ catalyst for CO oxidation, compared to Pt/Al_2O_3, to creation of catalytic sites localized at the interface between metallic Pt and ceria. It has been also reported [21] that addition of transition metal oxides (M: Cr, Mn, Fe, Co, Ni, Cu, Zn) on Al_2O_3 can improve the catalytic activity of Au in both low temperature CO oxidation and CH_4 oxidation reactions. In both cases the reaction was proposed to take place at the Au/MO_x perimeter [21]. Similar were the results reported by Wang et al. [26] for the low-temperature CO oxidation reaction over $Au/MO_x/Al_2O_3$ (M = Mn, Fe, Co, Ni, Cu) catalysts.

In our previous studies, over Pt/TiO_2 [19] and metal-promoted Pt/CeO_2 [20] catalysts, we presented spectroscopic (FTIR) evidence for the presence of a special kind of adsorption sites, at temperatures relevant to the WGS reaction. Adsorption of CO on these sites is characterized by FTIR peaks located at wavenumbers lower than that corresponding to Pt^0–CO species [19,20]. These sites, which are characterized by exceptional electron donating properties, have been assigned to platinum atoms interacting with Ti^{3+} or Ce^{3+} ions of titania or ceria, respectively, located at the metal/support interface [19,20,40–43]. It may be argued that similar sites may be present in all cases where platinum is in contact with a reducible support and also that their population and chemisorptive properties will depend on the crystallite size and redox properties of the reducible metal oxide.

Finally, it could be argued that the presence of reducible MO_x species may also affect the chemisoprtion properties and activity of dispersed platinum via the SMSI effect [44–46], which originates from migration of reduced suboxide species on the surface of Pt crystallites. This possibility should be probably excluded because of the relatively low reduction temperature used in this study. Migration of MO_x species is believed to occur during heat treatment typically above 773 K [44–46]. In addition, it is reported that the SMSI effect is not operable in the presence of water.

Summarizing, results of the present study provide strong evidence that the oxide support is directly involved in the WGS reaction mechanism and determines to a significant extent the activity of dispersed Pt crystallites as well as the apparent activation energy of the reaction. Composite supports, such as MO_x/Al_2O_3 or MO_x/TiO_2 investigated here, may be used to ''tune'' the WGS activity of dispersed noble metals by varying

MO_x nature, loading and crystallite size. Most probably, the same will be true for other catalytic reactions where reducibility of the support plays a determining role on catalytic activity.

5. Conclusions

The water-gas shift (WGS) activity of dispersed platinum depends strongly on the physicochemical characteristics of the metal oxide carrier, and is about 1–2 orders of magnitude higher when supported on ''reducible'' compared to ''irreducible'' metal oxides. Activity may be further improved when the metal oxide (MO_x) is dispersed on a high surface area support, such as Al_2O_3 or TiO_2, because reducibility increases with decreasing MO_x crystallite size. For composite $Pt/MO_x/Al_2O_3$ or $Pt/MO_x/TiO_2$ catalysts, the apparent activation energy and the reaction rate vary from one catalyst to another in a manner which depends on the nature, loading, and primary crystallite size of dispersed MO_x crystallites. Thereby, strong evidence is provided that the metal oxide support is directly involved in the WGS reaction mechanism. In particular, activity of $Pt/MO_x/Al_2O_3$ catalysts at 250 °C varies, depending on the nature of M in MO_x, in the order of $Ce > Co > Ti > Ho > Nd \approx Cu > Gd \approx La \approx Eu \approx Y \approx Zr > Ni > Sm > Tm > V > Er - Er > Fe > Cr \approx Mn > Al_2O_3$, with the rate (per gram of catalyst) for $Pt/CeO_x/Al_2O_3$ being about one order of magnitude higher, compared to that for Pt/Al_2O_3. Differences in activity become even larger if reaction rates are expressed per exposed Pt atom (TOF), in which case $Pt/MO_x/Al_2O_3$ catalysts containing rare earth metal oxides are generally much more active, compared to those containing oxides of the 3d transition metal elements. A similar effect is observed upon addition of MO_x (M = Ce, Nd, Co, Ho, Y, Gd) on Pt/TiO_2, which is the most active single-component catalyst investigated. $Pt/MO_x/TiO_2$ catalysts are generally more active and exhibit higher CO conversions at a given temperature, compared to $Pt/MO_x/Al_2O_3$ samples of the same MO_x nature and loading. Catalytic performance tests and kinetic measurements obtained under realistic feed compositions show that composite $Pt/MO_x/Al_2O_3$ and $Pt/MO_x/TiO_2$ catalysts are promising candidates for the development of active WGS catalysts suitable for fuel cell applications.

Acknowledgements

This work was funded by the General Secretariat of Research and Technology (GSRT) Hellas and the Commission of the European Community, under the PENED 2001 Programm (contract 01ED561).

References

[1] D.L. Trimm, Z.I. Önsan, Catal. Rev. 43 (2001) 31.
[2] A.F. Ghenciu, Curr. Opin. Solid State Mater. Sci. 6 (2002) 389.
[3] S.H. Chan, O.L. Ding, Int. J. Hydrogen Energy 30 (2005) 167.
[4] A. Qi, B. Peppley, K. Karan, Fuel Process. Technol. 88 (2007) 3.
[5] R. Burch, Phys. Chem. Chem. Phys. 8 (2006) 5483.
[6] Q. Fu, S. Kudriavtseva, H. Saltsburg, M. Flytzani-Stephanopoulos, Chem. Eng. J. 93 (2003) 41.
[7] D. Tibiletti, F.C. Meunier, A. Goguet, D. Reid, R. Burch, M. Boaro, M. Vicario, A. Trovarelli, J. Catal. 244 (2006) 183.
[8] D.C. Grenoble, M.M. Estadt, D.F. Ollis, J. Catal. 67 (1981) 90.
[9] J. Barbier Jr., D. Duprez, Appl. Catal. B 3 (1993) 61.
[10] R. Dictor, J. Catal. 106 (1987) 458.
[11] A. Basińska, L. Kępiński, F. Domka, Appl. Catal. A 183 (1999) 143.
[12] T. Bunluesin, R.J. Gorte, G.W. Graham, Appl. Catal. B 15 (1998) 107.
[13] Y. Li, Q. Fu, M. Flytzani-Stephanopoulos, Appl. Catal. B 27 (2000) 179.
[14] Q. Fu, H. Saltsburg, M. Flytzani-Stephanopoulos, Science 301 (2003) 935.
[15] M. Haruta, N. Yamada, T. Kobayashi, S. Iijima, J. Catal. 115 (1989) 301.
[16] J.M. Zalc, V. Sokolovskii, D.G. Löffler, J. Catal. 206 (2002) 169.
[17] P. Panagiotopoulou, D.I. Kondarides, J. Catal. 225 (2004) 327.
[18] P. Panagiotopoulou, D.I. Kondarides, Catal. Today 112 (2006) 49.
[19] P. Panagiotopoulou, A. Christodoulakis, D.I. Kondarides, S. Boghosian, J. Catal. 240 (2006) 114.
[20] P. Panagiotopoulou, J. Papavasiliou, G. Avgouropoulos, T. Ioannides, D.I. Kondarides, Water-gas shift activity of doped Pt/CeO_2 catalysts, Chem. Eng. J. (2007). doi:10.1016/j.cej.2007.03.054.
[21] R.J.H. Grisel, B.E. Nieuwenhuys, Catal. Today 64 (2001) 69.
[22] S. Khairulin, B. Béguin, E. Garbowski, M. Primet, J. Chem. Soc., Faraday Trans. 93 (1997) 2217.
[23] A. Ueda, M. Haruta, Appl. Catal. B 18 (1998) 115.
[24] A.C. Gluhoi, M.A.P. Dekkers, B.E. Nieuwenhuys, J. Catal. 219 (2003) 197.
[25] S. Damyanova, J.M.C. Bueno, Appl. Catal. A 253 (2003) 135.
[26] D. Wang, Z. Hao, D. Cheng, X. Shi, C. Hu, J. Mol. Catal. A 200 (2003) 229.
[27] Y.J. Mergler, A. van Aalst, J. van Delft, B.E. Nieuwenhuys, Appl. Catal. B 10 (1996) 245.
[28] M. Skoglundh, H. Johansson, L. Löwendahl, K. Jansson, L. Dahl, B. Hirschauer, Appl. Catal. B 7 (1996) 299.
[29] F.B. Noronha, M.A.S. Baldanza, R.S. Monteiro, D.A.G. Aranda, A. Ordine, M. Schmal, Appl. Catal. A 210 (2001) 275.
[30] H. Widjaja, K. Sekizawa, K. Eguchi, H. Arai, Catal. Today 47 (1999) 95.
[31] R.J.H. Grisel, C.J. Weststrate, A. Goossens, M.W.J. Crajé, A.M. van der Kraan, B.E. Nieuwenhuys, Catal. Today 72 (2002) 123.
[32] Y.J. Mergler, J. Hoebink, B.E. Nieuwenhuys, J. Catal. 167 (1997) 305.
[33] H. Cordatos, T. Bunluesin, J. Stubenrauch, J.M. Vohs, R.J. Gorte, J. Phys. Chem. 100 (1996) 785.
[34] S. Hilaire, X. Wang, T. Luo, R.J. Gorte, J. Wagner, Appl. Catal. A 215 (2001) 271.
[35] T. Shido, Y. Iwasawa, J. Catal. 141 (1993) 71.
[36] G. Jacobs, L. Williams, U. Graham, D. Sparks, B.H. Davis, J. Phys. Chem. B 107 (2003) 10398.
[37] C. Serre, F. Carin, G. Belot, C. Maire, J. Catal. 141 (1993) 1.
[38] H. Cordatos, D. Ford, R.J. Gorte, J. Phys. Chem. 100 (1996) 18128.
[39] E.S. Putna, B. Sherek, R.J. Gorte, Appl. Catal. B 17 (1998) 101.
[40] A. Yee, S.J. Morrison, H. Idriss, J. Catal. 191 (2000) 30.
[41] A. Bensalem, J.C. Muller, D. Tessier, F. Bozon-Verduraz, J. Chem. Soc. Faraday Trans. 92 (1996) 3233.
[42] O.S. Alexeev, S.Y. Chin, M.H. Engelhard, L. Ortiz-Soto, M.D. Amiridis, J. Phys. Chem. B 109 (2005) 23430.
[43] F. Boccuzzi, A. Chiorino, M. Manzoli, D. Andreeva, T. Tabakova, J. Catal. 188 (1999) 176.
[44] S. Tauster, S.C. Fung, L. Garten, J. Am. Chem. Soc. 100 (1978) 170.
[45] S.J. Tauster, S.C. Fung, J. Catal. 55 (1978) 29.
[46] G.L. Haller, D.E. Resasco, Adv. Catal. 36 (1989) 173.